Fast manipulation of spin-wave excitations in an atomic ensemble

Zhongxiao Xu, Yuelong Wu, Hailong Liu, Shujing Li, and Hai Wang*

The State Key Laboratory of Quantum Optics and Quantum Optics Devices, Institute of Opto-Electronics, Shanxi University, Taiyuan 030006, People's Republic of China

(Received 3 May 2012; revised manuscript received 8 April 2013; published 26 July 2013)

We experimentally demonstrated a fast manipulation of two orthogonal spin-wave excitations in an ensemble of cold ^{87}Rb atoms. The spin-wave manipulation is realized by transferring the excitations between two collective states, and a π rotation between the two spin waves is accomplished on a time scale of $\sim$100 ns. The multiple π rotations are completed based on the single π rotation. The results show that the retrieval optical signal from the manipulated spin waves gradually decreases along with the increasing of π-rotation numbers. The loss mechanism of spin waves caused by a Raman π rotation is simply analyzed, and the possible methods to mitigate the loss are discussed. Using multiple π rotations, one can implement the dynamical decoupling to protect the qubit memory in an atom ensemble from the influence of environmental noise.

DOI: 10.1103/PhysRevA.88.013423 PACS number(s): 32.80.Qk, 03.67.−a, 42.50.Ex, 42.50.Gy

I. INTRODUCTION

The optical memory based on electromagnetically induced transparency (EIT) or the spontaneous Raman process in atomic ensembles provides a physical platform for the implementation of quantum repeater protocols [1–3]. Since numerous atoms can realize the collectively enhanced coupling to a certain optical mode, the retrieval optical signal from the atomic ensemble can be emitted in a well-defined direction with high probability [4,5]. For a typical EIT three-level Λ-type atomic system in an atomic Mott insulator [6] or BEC [7], a light pulse can be transferred into a spin wave and can be stored in an atomic ensemble with a very long lifetime. For storing an arbitrary polarization photon in an atomic ensemble to construct a qubit memory, the two collective spin waves (dark polaritons) are required [5,8]. The experimental studies on spin-wave qubit memories of atomic ensembles based on spontaneous Raman scattering [9–12] and EIT storage schemes [13–15] have been achieved. Quantum information processing (QIP) schemes involving single-bit operations and using the qubit memory of atomic ensembles have been proposed [16,17]. The single-qubit rotations have been realized in a single trapped ion [18] and neutral atom [19] in which qubits are encoded into a pair of ground-state hyperfine sublevels (internal states) as well as Raman laser pulses, or microwave pulses are applied to coherently manipulate populations between internal states, respectively. After the manipulations are completed, the populations in the internal states are measured by detecting fluorescence within a solid angle. As for the manipulation of spin waves, the transfer of spin coherences from the initial memory channel to a target channel has also been experimentally demonstrated in a BEC [7] and an atomic vapor cell [20], respectively. However, the Ramsey fringes or Rabi oscillations between the two spin waves have not been observed in these experiments. In 2011, a significant experiment for the manipulation of spin waves in an atomic ensemble was realized [21]. The atoms are prepared in initial ground state $5S_{1/2}|F=1,m_F=1\rangle$ first, and then a circularly polarized signal light pulse is stored in the ensemble by EIT. The storage corresponds to a coherent transfer of a few atoms from ground state $|F=1,m_F=1\rangle$ to "excited" state $5S_{1/2}|F=2,m_F=1\rangle$, i.e., a generation of a spin wave. Successively, by applying a Raman pulse to the atoms, the coherent rotation and the Rabi oscillations between two components of the spin wave are demonstrated [21].

Here, we present the experimental demonstration of the fast manipulation of two orthogonal spin-wave excitations in an atomic ensemble. Although the generation scheme of the spin wave in the present paper and Ref. [21] is the same, the manipulated quantum state is not identical. In Ref. [21] the spin wave is manipulated by transferring the atomic population of ground state $|F=1,m_F=1\rangle$ into the other ground state $|F=1,m_F=-1\rangle$. However, in the now-presented experiment the spin-wave manipulation is realized by transferring the atomic population of excited state $|F=2,m_F=1\rangle$ into state $|F=2,m_F=-1\rangle$. Therefore, the achieved manipulation can be named as the manipulation of the spin-wave excitations, which has some special applications. Such as, it can be utilized to realize the dynamic decoupling [22] for protecting the spin-wave qubits [9,23] in the atomic ensemble against the environment-induced dephasing, whereas, the manipulation of the spin-wave ground state discussed in Ref. [21] is not able to be used for realizing this task. Besides, we achieve some experimental measurements, which have not been implemented in Ref. [21]: (1) The multiple π rotations between two spin waves are demonstrated. (2) The dependence of the retrieval signals from the spin waves upon $n\,\pi$ pulses is observed. (3) The dephasing time of the spin waves caused by the fluctuation in the magnetic field is measured by observing the damped Ramsey fringes.

This paper is organized as follows. In Sec. II, we simply introduce the theories about the storage, Raman manipulations, and retrieval processes for two spin waves. In Sec. III, we describe the experimental setup for the fast manipulation of spin-wave excitations in an atomic ensemble. The experimental implementations and results are given in Sec. IV. The physical reasons for the spin-wave decoherence during Raman transfers are analyzed, and the possible methods for suppressing the decoherence are discussed in Sec. V. At last, a brief conclusion is given in Sec. VI.

*Corresponding author: wanghai@sxu.edu.cn

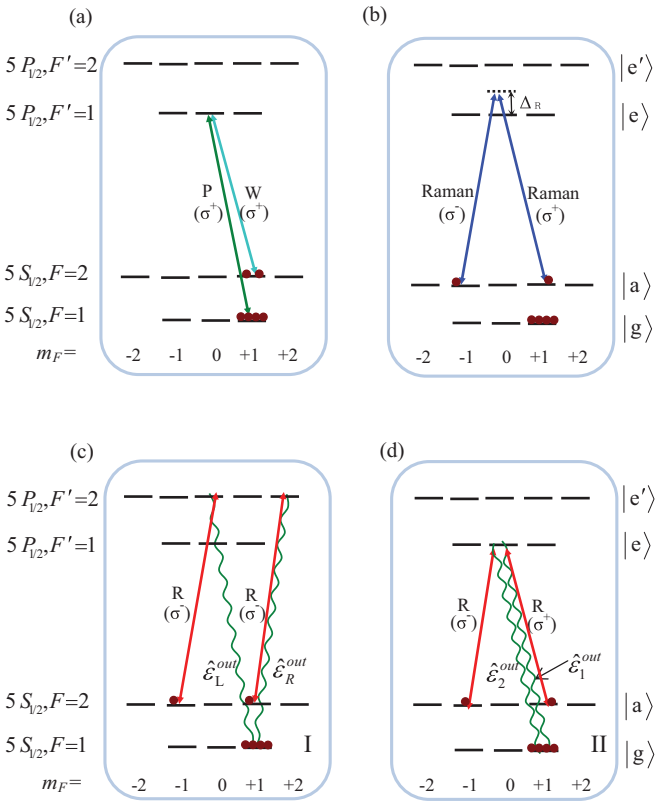

FIG. 1. (Color online) (a) The atomic levels of the ^{87}Rb atom for optical storage, (b) Raman manipulation, (c) reading scheme I, and (d) reading scheme II. R, W, and P denote reading, writing, and signal laser beams, respectively. σ^+ and σ^- denote the left- and right-circularly polarized light, respectively.

II. THEORETICAL MODEL

The relevant levels of the ^{87}Rb atoms in Fig. 1 are defined as $|g\rangle = |5S_{1/2}, F = 1\rangle$, $|a\rangle = |5S_{1/2}, F = 2\rangle$, $|e\rangle = |5P_{1/2}, F' = 1\rangle$, and $|e'\rangle = |5P_{1/2}, F' = 2\rangle$, respectively. The atomic spin wave associated with the $|g_{m_F=1}\rangle \leftrightarrow |a_{m_F=1}\rangle$ coherence can be described by a collective and slowly varying atomic operator, which is an appropriate average over a small but macroscopic volume with atomic numbers of $N_z \gg 1$ at positions z [24,25],

$$\tilde{\rho}_{1,1}(z,t) = (N_z)^{-1} \sum_{j=1}^{N_z} |a_{m_F=1}\rangle_{jj}\langle g_{m_F=1}| e^{i\omega_a t}, \tag{1}$$

where m_F is the magnetic quantum number, ω_a is the frequency of the transition $|g\rangle \leftrightarrow |a\rangle$, and $|g_{m_F=1}\rangle(|a_{m_F=1}\rangle)$ denotes the Zeeman sublevel $|5S_{1/2}, F = 1, m_F = 1\rangle(|5S_{1/2}, F = 2, m_F = 1\rangle)$. The initial spin wave $\tilde{\rho}_{1,1}(z,t)$ is created by storing a right-circularly (σ^+)-polarized optical signal field $\hat{\varepsilon}_+^{\rm in}(z,t)$ into the atomic ensemble with an EIT scheme. As shown in Fig. 1(a), a weak signal field $\hat{\varepsilon}_+^{\rm in}(z,t)$ couples to the transition $|g_{m_F=1}\rangle \leftrightarrow |e_{m_F=0}\rangle$, and a σ^+-polarized writing control field couples to the transition $|a_{m_F=1}\rangle \leftrightarrow |e_{m_F=0}\rangle$. Before the storage, we prepare all atoms in state $|g_{m_F=1}\rangle$. By switching off the writing beam at time t_0, the signal light pulse will be decelerated and then will be mapped onto the spin wave according to

$$\hat{\varepsilon}_+^{\rm in}(z,t_0) \rightarrow \tilde{\rho}_{1,1}(z,t_0). \tag{2}$$

Such a mapping can be well described by the theory of the dark-state polariton [24,25]. Actually, the generation of the spin wave $\tilde{\rho}_{1,1}(z,t_0)$ corresponds to the transfer of a few atoms from initial state $|g_{m_F=1}\rangle$ to state $|a_{m_F=1}\rangle$. Assuming that the weak signal field $\hat{\varepsilon}_+^{\rm in}(z,t)$ is a coherent state $|P\rangle = \sum_n c_n|n\rangle$ [where $|n\rangle$ are number states of the optical field $\hat{\varepsilon}_+^{\rm in}(z,t)$], the storage process can be written as the following transformation [26]:

$$\sum c_n|n\rangle|g_{m_F=1}\rangle \rightarrow |0\rangle|d_+\rangle, \tag{3}$$

where $|d_+\rangle = \sum c_n|a^n_{m_F=1}\rangle$ is the superposition of collective states $|a^n_{m_F=1}\rangle(n = 1,2,3,\ldots)$ containing n atoms (excitations) in the level $|a_{m_F=1}\rangle$ and can be written as symmetric Dicke-like states,

$$|a^0_{m_F=1}\rangle = |g_{m_F=1}\rangle = |g^1_{m_F=1},\ldots,g^N_{m_F=1}\rangle, \tag{4a}$$

$$|a^1_{m_F=1}\rangle = \frac{1}{\sqrt{N}} \sum_{i=1}^{N} |g^1_{m_F=1},\ldots,a^i_{m_F=1},\ldots,g^N_{m_F=1}\rangle, \tag{4b}$$

$$|a^2_{m_F=1}\rangle = \frac{1}{\sqrt{2!N(N-1)}} \sum_{i\neq j=1}^{N} |g^1_{m_F=1},\ldots,a^i_{m_F=1},\ldots,a^j_{m_F=1}\ldots,g^N_{m_F=1}\rangle, \tag{4c}$$

$$|a^3_{m_F=1}\rangle = \frac{1}{\sqrt{3!N(N-1)(N-2)}} \sum_{i\neq j\neq k=1}^{N} |g_{m_F=1},\ldots,a^i_{m_F=1},\ldots,a^j_{m_F=1},\ldots,a^k_{m_F=1},\ldots,g^N_{m_F=1}\rangle, \text{etc.}, \tag{4d}$$

with N as the number of atoms. By using the Raman transfer scheme, we may coherently rotate the collective excitations between states $|a_{m_F=1}\rangle$ and $|a_{m_F=-1}\rangle$. The Raman laser is a linearly polarized light field $E_R(t) = E_{R_0}e^{-i\omega_R t}$, which provides σ^+- and σ^-- (left- and right-) circularly polarized light fields $E_{R+}(t) = E_{R_0^+}\binom{1}{-i}e^{-i\omega_R t}$ and

$E_{R-}(t) = E_{R_0^-}(\begin{smallmatrix}1\\ i\end{smallmatrix})e^{-i\omega_R t}$, where $E_{R_0^+} = E_{R_0^-} = E_{R_0}/2$. The σ^+- (σ^-)− polarized fields simultaneously couple to the transition $|a_{m_F=1}\rangle \leftrightarrow |e_{m_F=0}\rangle$($|a_{m_F=-1}\rangle \leftrightarrow |e_{m_F=0}\rangle$) with a single-photon detuning $\Delta_1 = \Delta_R$ and the transition $|a_{m_F=1}\rangle \leftrightarrow |e'_{m_F=0}\rangle$ ($|a_{m_F=-1}\rangle \leftrightarrow |e'_{m_F=0}\rangle$) with a single-photon detuning $\Delta_2 = \omega_{12} - \Delta_R$ ($\omega_{12} = 816$ MHz is the hyperfine splitting of $5P_{1/2}F' = 1$ and $F' = 2$) [27], respectively. In the presented experiment, the single-photon detuning Δ_R and/or $\omega_{12} - \Delta_R$ are much larger than the natural linewidth Γ and the resonant Rabi frequencies, thus, an effectively Raman transition between states $|a_{m_F=-1}\rangle$ and $|a_{m_F=1}\rangle$ will be obtained. The Raman-Rabi frequency can be written as [28]

$$\Omega_R = \frac{\Omega_+\Omega_-}{\Delta_R} + \frac{\Omega'_+\Omega'_-}{\omega_{12} - \Delta_R}, \tag{5}$$

where $\Omega_\pm = \mu_\pm E_{R_0^\pm}/h$ and $\Omega'_\pm = \mu'_\pm E_{R_0^\pm}/h$ are the resonant one-photon Rabi frequencies, $\mu_\pm$ and $\mu'_\pm$ are the dipole moments for the transitions $|e_{m_F=0}\rangle \leftrightarrow |a_{m_F=\pm1}\rangle$ and $|e'_{m_F=0}\rangle \leftrightarrow |a_{m_F=\pm1}\rangle$, respectively. For ^{87}Rb atoms [29], we have

$$\mu_+ = \mu_- = \mu'_+ = \mu'_- = \mu_0 = \frac{1}{\sqrt{4}}\langle J = 1/2\|er\|J' = 1/2\rangle, \tag{6a}$$

and

$$\Omega_+ = \Omega_- = \Omega'_+ = \Omega'_- = \Omega_{R0} \qquad \left(\Omega_{R0} = \mu_0 E_{R_0^\pm}/h\right). \tag{6b}$$

If the jth atom is excited to state $|a^j_{m_F=1}\rangle$ during the storage process, it will evolve to the coherent superposition state $|\Phi^j\rangle = \alpha|a^j_{m_F=1}\rangle + e^{-i\varphi}\beta|a^j_{m_F=-1}\rangle$ after the Raman transfer where the probability amplitudes $\alpha = \cos(\Omega_R t/2)$ and $\beta = \sin(\Omega_R t/2)$, t is the interaction time of the Raman laser and the atoms, and $\varphi = \varphi_+ - \varphi_-$ is the phase difference between the Raman fields E_{R+} and E_{R-} [21]. So, the initial collective atomic state $|\Psi(t_0)\rangle = \sum c_n|a^n_{m_{F=1}}\rangle = |d_+\rangle$ will be transferred into the coherent superposition state $|\Psi(t)\rangle = \alpha|d_+\rangle + e^{-i\varphi}\beta|d_-\rangle$, where $|d_-\rangle = \sum c_n|a^n_{m_F=-1}\rangle$ is a superposition of the collective states $|a^n_{m_F=-1}\rangle$. Correspondingly, the initial spin wave $\tilde{\rho}_{1,1}(z,t)$ will be transferred into the superposition $\tilde{\rho}_{\Phi,1}(z,t) = \alpha\tilde{\rho}_{1,1}(z,t) + e^{-i\varphi}\beta\tilde{\rho}_{-1,1}(z,t)$ after the Raman manipulation, where $\tilde{\rho}_{\Phi,1}(z,t) = \frac{1}{N_z}\sum_{j=1}^{N_z}|\Phi^j\rangle\langle g^j_{m_F=1}|$ and $\tilde{\rho}_{-1,1}(z,t) = \frac{1}{N_z}\sum_{j=1}^{N_z}|a^j_{m_F=-1}\rangle\langle g^j_{m_F=1}|e^{i\omega_a t}$ are the spin waves associated with $|\Phi\rangle \leftrightarrow |g_{m_F=1}\rangle$ and $|a_{m_F=-1}\rangle \leftrightarrow |g_{m_F=1}\rangle$ coherences. Since the two spin waves $\tilde{\rho}_{1,1}(z,t)$ and $\tilde{\rho}_{-1,1}(z,t)$ are orthogonal to each other, they form a spin-wave basis. In this basis, the spin wave $\tilde{\rho}_{\Phi,1}(z,t)$ may be rewritten as a vector,

$$\vec{S}_{\Phi,1}(z,t) = \vec{S}_{1,1} + \vec{S}_{-1,1} = \langle|\tilde{\rho}_{\Phi,1}(z,t)|\rangle\begin{pmatrix}\alpha\\ e^{-i\phi}\beta\end{pmatrix}, \tag{7}$$

where $\vec{S}_{1,1}(z,t) = \langle|\tilde{\rho}_{\Phi,1}(z,t)|\rangle(\begin{smallmatrix}\alpha\\ 0\end{smallmatrix})$ and $\vec{S}_{-1,1}(z,t) = \langle|\tilde{\rho}_{\Phi,1}(z,t)|\rangle(\begin{smallmatrix}0\\ e^{-i\phi}\beta\end{smallmatrix})$ are the vectors of spin waves $\tilde{\rho}_{1,1}(z,t)$ and $\tilde{\rho}_{-1,1}(z,t)$, respectively. Since in our experiment only a few atoms are transferred into state $|a_{m_F=1}\rangle$ during the storage process, we may assume that the population of the atoms in state $|g_{m_F=1}\rangle$ is $\rho_{g_{m_F=1},g_{m_F=1}} \approx 1$. Thus, the population of spin wave $\vec{S}_{\Phi,1}(z,t)$ can be calculated by $\langle|\tilde{\rho}_{\Phi,1}(z,t_0)|^2\rangle = \langle\tilde{\rho}_{\Phi,1}(t_0)\tilde{\rho}^+_{\Phi,1}(t_0)\rangle = \langle\tilde{\rho}_{1,1}(t_0)\rho^+_{1,1}(t_0)\rangle \approx \langle\rho_{a_{m_F=1},a_{m_F=1}}(t_0)\rangle$, where $\rho_{a_{m_F=1},a_{m_F=1}}(t_0)$ is the number of atoms coherently transferred into state $|a_{m_F=1}\rangle$ during the storage.

The manipulated spin waves will be converted into the retrieval optical signal when a controlling reading beam is switched on. Under the conditions of collective enhancement, the retrieval signal field is emitted with high efficiency into a certain direction determined by the phase-match condition (PMC) $\vec{k}_s - \vec{k}_w = \vec{k}_{rs} - \vec{k}_r$, where $\vec{k}_s$, $\vec{k}_w$, $\vec{k}_r$, and $\vec{k}_{rs}$ are the wave vectors of the signal, writing, reading, and retrieval signal fields [4,5,11,30]. Under the experimental condition of $\vec{k}_w = \vec{k}_r$, we have $\vec{k}_s = \vec{k}_{rs}$, which means that the retrieval signal field propagates along the direction of the input signal field. During the experiment, we use the following two reading schemes to retrieve the stored signals:

(1) In reading scheme I [see Fig. 1(c)], we apply a σ^--polarized reading beam with the frequency tuned to transition $|5S_{1/2}, F = 2\rangle \leftrightarrow |5P_{1/2}, F' = 2\rangle$ to read the spin waves. In this case, spin waves $\vec{S}_{1,1}(z,t)$ and $\vec{S}_{-1,1}(z,t)$ are converted into σ^-- and σ^+-polarized optical fields $\varepsilon_R^{\rm out}(z,t)$ and $\varepsilon_L^{\rm out}(z,t)$, respectively, and thus, the mapping between the spin-wave qubit and the photonic qubit is realized. Such conversion is described by the two dark-state polaritons [8],

$$\hat{\Psi}_R(z,t) = \cos\ \vartheta_+\hat{\varepsilon}_R^{\rm out}(z,t) - \sin\ \vartheta_+\sqrt{N}\vec{S}_{1,1}(z,t), \tag{8a}$$

$$\hat{\Psi}_L(z,t) = \cos\ \vartheta_-\hat{\varepsilon}_L^{\rm out}(z,t) - \sin\ \vartheta_-\sqrt{N}\vec{S}_{1,1}(z,t), \tag{8b}$$

where $\vartheta_+ = \arctan\frac{G\sqrt{N}}{\Omega_{C+}}$ and $\vartheta_- = \arctan\frac{G\sqrt{N}}{\Omega_{C-}}$ are the mixed angles of the two dark-state polaritons; Ω_{C+} and Ω_{C-} are the Rabi frequencies of the σ^--polarized reading beam for transitions $|a_{m_F=-1}\rangle \leftrightarrow |e'_{m_F=0}\rangle$ and $|a_{m_F=1}\rangle \leftrightarrow |e'_{m_F=2}\rangle$, respectively; G is the atom-field coupling constant. For a strong reading field $\Omega^2_{C\pm} \gg G\sqrt{N}$, i.e.,$\vartheta_+ \approx \vartheta_- \approx 0$, the two polaritons will become pure optical fields [25],

$$\hat{\varepsilon}^{\rm out}(z,t) = \begin{pmatrix}\hat{\varepsilon}_L^{\rm out}(z,t)\\ \hat{\varepsilon}_R^{\rm out}(z,t)\end{pmatrix} \propto \sqrt{N}\langle|\tilde{\rho}_{\Phi,1}(z,t_0)|\rangle\begin{pmatrix}\sqrt{\eta_+}\alpha\\ \sqrt{\eta_-}e^{-i\varphi}\beta\end{pmatrix}. \tag{9}$$

From Eq. (8), one can find that the dark states do not contain the excited states, so the conversions between photonic state and spin waves are immune to spontaneous emission. The retrieval efficiency $\eta_+(\eta_-)$ mainly depends on the optical depth of the signal transition $|g_{m_F=1}\rangle \leftrightarrow |e_{m_F=1}\rangle$($|g_{m_F=1}\rangle \leftrightarrow |e_{m_F=-1}\rangle$) [31]. Since the dipole moment for transitions $|g_{m_F=1}\rangle \leftrightarrow |e_{m_F=1}\rangle$ and $|g_{m_F=1}\rangle \leftrightarrow |e_{m_F=-1}\rangle$ are asymmetric, η_+ and η_- are not the same. Thus, the retrieval signal from spin wave $\vec{S}_{1,1}(z,t)$ is different from that from $\vec{S}_{-1,1}(z,t)$ even when their populations are identical (i.e., $|\alpha|^2 = |\beta|^2$).

(2) When $|\alpha|^2 = |\beta|^2$, we can use another reading scheme to make the efficiencies of the retrieval optical signals from $\vec{S}_{1,1}(z,t)$ and $\vec{S}_{-1,1}(z,t)$ be symmetric, and based on it, the Raman transfer efficiency can be accurately measured. In the scheme [see Fig. 1(d)], the σ^+- or σ^--polarized beam with the frequency tuned to transition $|5S_{1/2}, F = 2\rangle \leftrightarrow |5P_{1/2}, F' = 1\rangle$ is utilized as the reading beam for retrieving the σ^+-optical field $\hat{\varepsilon}_1(z,t)$ or $\hat{\varepsilon}_2(z,t)$ from spin wave $\vec{S}_{1,1}(z,t)$ or $\vec{S}_{-1,1}(z,t)$, which can be described by the generalized

dark-state polariton [32,33],

$$\hat{\Psi}(z,t) = \cos\vartheta\,\hat{\varepsilon}(z,t) - \sin\vartheta\sqrt{N} \times \left(\frac{\Omega_1}{\sqrt{\Omega_1^2+\Omega_2^2}}\tilde{\rho}_{1,1}(z,t) + \frac{\Omega_2}{\sqrt{\Omega_1^2+\Omega_2^2}}\tilde{\rho}_{-1,1}(z,t)\right), \tag{10}$$

where the mixed angle is $\vartheta(t) = \arctan\frac{G\sqrt{N}}{\sqrt{\Omega_1^2+\Omega_2^2}}$ and Ω_1 and Ω_2 are the Rabi frequencies for the σ^+- and σ^--polarized reading beams, respectively. For a strong reading field $\Omega_1 \gg G\sqrt{N}$ or $\Omega_2 \gg G\sqrt{N}$, i.e., $\vartheta \approx 0$, the generalized dark-state polariton will become the retrieved optical field $\hat{\varepsilon}_1(z,t)$ or $\hat{\varepsilon}_2(z,t)$,

$$\hat{\varepsilon}_1(z,t) \propto \sqrt{N}\langle|\tilde{\rho}_{\Phi,1}(z,t_0)|\rangle\sqrt{\eta}\begin{pmatrix}\alpha\\0\end{pmatrix}, \tag{11a}$$

or

$$\hat{\varepsilon}_2(z,t) \propto \sqrt{N}\langle|\tilde{\rho}_{\Phi,1}(z,t_0)|\rangle\sqrt{\eta}\begin{pmatrix}0\\e^{-i\varphi}\beta\end{pmatrix}, \tag{11b}$$

where we have assumed that the retrieval efficiencies for fields $\hat{\varepsilon}_1(z,t)$ and $\hat{\varepsilon}_2(z,t)$ are the same and are equal to η since transitions $|a_{m_F=1}\rangle \leftrightarrow |e_{m_F=0}\rangle$ and $|a_{m_F=-1}\rangle \leftrightarrow |e_{m_F=0}\rangle$ are symmetric.

III. EXPERIMENTAL SETUP

The experimental setup is shown in Fig. 2(a). A cold atomic cloud including about 10^8 ^{87}Rb atoms serves as the atomic ensemble. The measured optical depth of the cold atoms is about 1.5 under the magneto-optical trap (MOT) temperature of ~200 μK. The involved atomic levels in the population preparation are shown in Fig. 2(b). The σ^--polarized pumping laser of 780 nm coupled to transition $|5S_{1/2}, F=1\rangle \leftrightarrow |5P_{3/2}, F'=1\rangle$ and the σ^--polarized pumping laser of 795 nm coupled to transition $|5S_{1/2}, F=2\rangle \leftrightarrow |5P_{1/2}, F'=2\rangle$ serve as pumps 1 and 2, respectively. The σ^+-polarized writing beam W (with a power of ~1 mW and a diameter of 2 mm) is tuned to transition $|a_{m_F=1}\rangle \leftrightarrow |e_{m_F=0}\rangle$ and goes through the cold atoms with a small deviation angle of ~0.4° from $\hat{z}$ ($\hat{z}$ is the unit vector in the z direction). The σ^+-polarized optical signal field $\hat{\varepsilon}_+^{\rm in}(z,t)$ (with a power of ~17 μW and a diameter of 1 mm) is tuned to transition $|g_{m_F=1}\rangle \leftrightarrow |e_{m_F=1}\rangle$ and goes through the cold atoms along $\hat{z}$. The horizontally polarized Raman laser beam (with an ~4.5-mm diameter) passes through the cold atoms with a deviation angle of ~1° from $\hat{z}$. We use an analog acousto-optic modulator to modulate the Raman laser amplitude and then obtain a rectangular pulse with a variable time length. The manipulated spin waves are retrieved by applying a reading beam with a power of ~17.7 mW and a diameter of ~2.5 mm. The time sequence of an experimental cycle is shown in Fig. 2(c). Switching off the MOT and waiting for 1 ms while the MOT magnetic field decays to zero, we then apply a dc magnetic field B_0 along $\hat{z}$ to define the quantization axis. After 0.37 ms, the magnetic field $B_0\hat{z}$ is fixed at ~300 mG, and the pumps 1 and 2 as well as the writing laser beams are switched on to prepare the atoms into the desired ground state $|g_{m_F=1}\rangle$. After about 20 μs, pumps 1 and 2 are turned off, and the σ^+-polarized signal pulse (with a pulse length of 200 ns) is injected into the atom ensemble. At the falling edge of

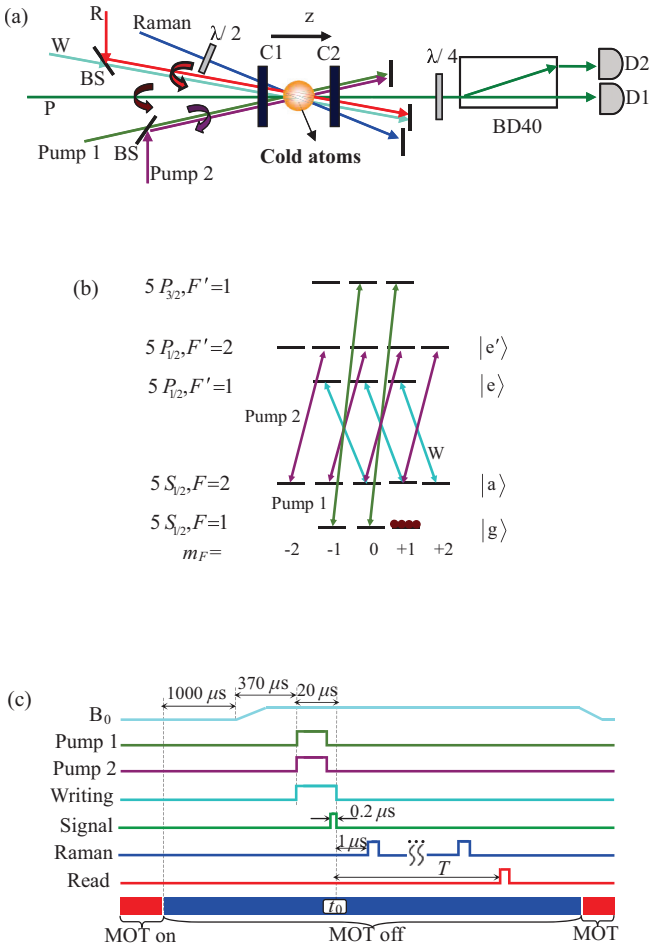

FIG. 2. (Color online) (a) Experimental setup. BS: beam splitter; C1 and C2: axial magnetic coils; PBS: polarization beam splitter; D1 and D2: photodetectors; and BD40: beam displacer. (b) The involved atomic levels in population preparation. (c) Time sequence of an experimental cycle.

the signal pulse [corresponding to $t_0 = 0$ in Fig. 2(c)], the σ^+-writing laser beam is ramped to zero, and thus, the signal pulse is stored into the atomic ensemble to create an initial spin wave $\rho_{1,1}(z,t_0)$. After a delay time of $t = 1$ μs, we begin to apply a Raman laser pulse to rotate the stored spin waves. Finally, the manipulated spin waves are retrieved by switching on the reading beam after a storage time T. The retrieved σ^+- and/or σ^--polarized signals propagate along $\hat{z}$ and become vertically (horizontally) polarized light after passing through a $\lambda/4$-wave plate. They are split by a BD and are detected by detectors D1 and D2 (Newfocus 1801), respectively.

IV. EXPERIMENTAL IMPLEMENTION AND RESULTS

Before Raman manipulations, we measure total storage-retrieval efficiencies $\eta_{0,I}$ and $\eta_{0,II}$, which are defined as $\eta_{0,I} = \frac{\int\langle|\hat{\varepsilon}_0^{{\rm out},I}(z,t)|\rangle^2 dt}{\int\langle|\hat{\varepsilon}_+^{\rm in}(z,t)|\rangle^2 dt}$ and $\eta_{0,II} = \frac{\int\langle|\hat{\varepsilon}_0^{{\rm out},II}(z,t)|\rangle^2 dt}{\int\langle|\hat{\varepsilon}_+^{\rm in}|(z,t)\rangle^2 dt}$, respectively, where $\int\langle|\varepsilon_0^{{\rm out},I}(t)|\rangle^2 dt (\int\langle|\varepsilon_0^{{\rm out},II}(t)|\rangle^2 dt)$ corresponds to the retrieved photon number of the σ^+- polarized field from the

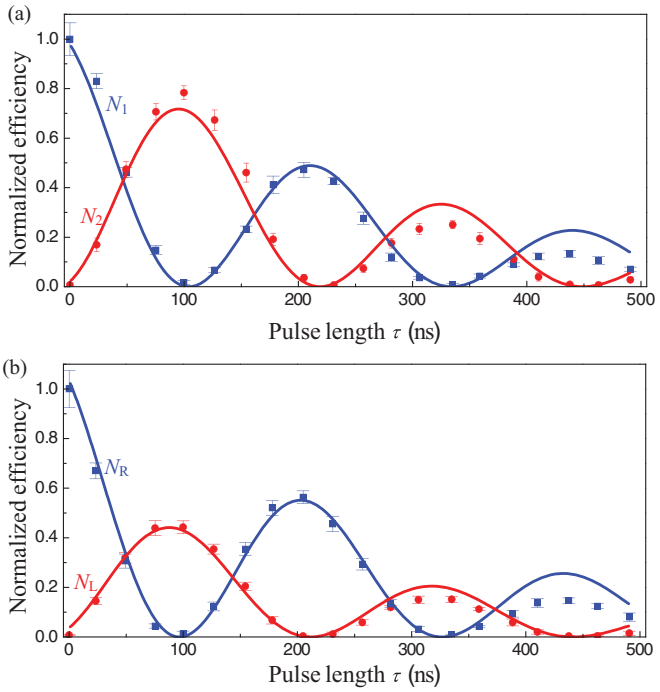

FIG. 3. (Color online) (a) Normalized retrieval efficiencies (N_1 and N_2) as a function of the Raman pulse length τ. The solid lines are exponential fits to the data. (b) Normalized retrieval efficiencies (N_R and N_L) as a function of the Raman pulse length τ. The solid lines are exponential fits to the data.

initial spin wave $\tilde{\rho}_{1,1}(z,t_0)$ by means of read scheme I (II). The retrieval optical signals are collected and are detected along the PMC direction ($\hat{z}$). The measured values of $\eta_{0,I}$ and $\eta_{0,II}$ are ~13% and ~9% respectively, for the storage time of $T = 28.9\ \mu$s, which show that the spin coherences are well preserved.

By applying Raman laser pulses with a fixed peak power of $P = 80$ mW and a variable time length of $\tau = 0 - 500$ ns, we demonstrate Rabi oscillations between the two spin waves and measure the maximum Raman transfer efficiency. First, we observe such Rabi oscillations by measuring the retrieval signals $\hat{\varepsilon}_1^{\text{out}}(z,t)$ and $\hat{\varepsilon}_2^{\text{out}}(z,t)$, respectively, with reading scheme II. In the scheme, the readouts are in two separate time-sequence cycles, respectively. To describe the relative values of readout fields $\hat{\varepsilon}_1^{\text{out}}(z,t)$ and $\hat{\varepsilon}_2^{\text{out}}(z,t)$, respectively, to the original $\hat{\varepsilon}_0^{\text{out}}(z,t)$ readout, we define the normalized retrieval efficiencies $N_{1(2)} = \frac{\int \langle|\hat{\varepsilon}_{1(2)}^{\text{out}}(z,t)|\rangle^2 dt}{\int \langle|\hat{\varepsilon}_0^{\text{out},II}(z,t)|\rangle^2 dt}$, where $\int \langle|\hat{\varepsilon}_{1(2)}^{\text{out}}(z,t)|\rangle^2 dt$ is the retrieval photon number from the Raman manipulated spin wave $\vec{S}_{1,1}(z,t)[\vec{S}_{-1,1}(z,t)]$. The squares (circles) in Fig. 3(a) are the measured dependence of the normalized retrieval efficiencies $N_1(N_2)$ upon the Raman pulse length τ, which represent the damped Rabi oscillations between the two spin waves. The achieved π-rotation time is $\tau \approx 100$ ns, corresponding to a Rabi frequency of $\Omega_R \approx 4.4$ MHz. The decay of the spin waves induced by the Raman manipulation is significant, and at first period ($\tau \approx 100$ ns) the normalized retrieval efficiency N_2 decreases to ~0.784, which corresponds to a π-pulse fidelity of ~78.4%. The solid curves N_1 and N_2 are the fits to the experimental data based on functions $(1 + \cos\ \Omega_R\tau)e^{-\tau/\tau_0}/2$ and $(1 - \cos\ \Omega_R\tau)e^{-\tau/\tau_0}/2$, respectively, with a $1/e$ decay time of $\tau_0 \approx 300$ ns. Here, the Rabi oscillations of retrieval signals tend to a very low level, and the result is different from that of a single atomic qubit for which the decoherence of the damped Rabi oscillations only reach about 50% [34]. That is because the decoherence mechanisms and the readout ways for the spin-wave qubits and the single atomic qubits are different. For the discussed spin-wave qubit memory, there are two types of decoherence mechanisms: (1) the dephasing between the two spin waves, which comes from the random phases induced by fluctuations of the magnetic field. It plays the same role as the decoherence in a single atomic qubit. (2) The decoherence of a spin wave itself, which dominantly derives from the coherence loss of the spin wave during Raman transfers. The lost coherence of the spin wave will not be mapped into the retrieval signal emitting into the PMC direction, and the losses will increase when the observation time is prolonged. Thus, the Rabi oscillations of the retrieval signals will tend to the zero level along with the observed time.

Subsequently, we observe the Raman transfer by measuring the retrieval signals $\hat{\varepsilon}_R^{\text{out}}(z,t)$ and $\hat{\varepsilon}_L^{\text{out}}(z,t)$ via reading scheme I. The normalized retrieval efficiencies $N_{R(L)}$ of the signals $\hat{\varepsilon}_{R(L)}^{\text{out}}(z,t)$ relative to the original readout $\hat{\varepsilon}_0^{\text{out},I}(z,t)$ are defined as

$$N_{R(L)} = \frac{n_{R(L)}}{n_{0,I}} = \frac{\int \langle|\hat{\varepsilon}_{R(L)}^{\text{out}}(z,t)|\rangle^2 dt}{\int \langle|\hat{\varepsilon}_0^{\text{out},I}(z,t)|\rangle^2 dt}, \tag{12}$$

where $\int \langle|\hat{\varepsilon}_{R(L)}^{\text{out}}(z,t)|\rangle^2 dt$ corresponds to the number of retrieval photons from the Raman manipulated spin wave $\vec{S}_{1,1}(z,t)[\vec{S}_{-1,1}(z,t)]$. The squares (circles) in Fig. 3(b) are the normalized retrieval efficiencies $N_{R(L)}$ as the function of duration τ of the Raman pulse, which also express the damped Rabi oscillations with a π-rotation time of 100 ns. The solid curves N_R and N_L in Fig. 3(b) are the fits to the experimental data based on functions $(1 + \cos\ \Omega_R\tau)e^{-\tau/\tau_0}/2$ and $\zeta(1 - \cos\ \Omega_R\tau)e^{-\tau/\tau_0}/2$, respectively. The used values of $1/e$ decay time τ_0 and Rabi frequency Ω_R in the fits are 300 ns and 4.4 MHz, respectively, which are consistent with the corresponding values used in the fittings to the data in Fig. 3(a). Such consistency shows that spin waves $\vec{S}_{1,1}(z,t)$ and $\vec{S}_{-1,1}(z,t)$ are well transferred into the retrieval signals N_1 and N_2 (N_R and N_L), respectively, in reading scheme I (II). The used parameter $\zeta = \frac{N_L}{N_R} = 0.53$ in the fittings of Fig. 3(b) is not equal to 1, which means that the retrieval efficiencies for the two spin waves $\vec{S}_{1,1}(z,t)$ and $\vec{S}_{-1,1}(z,t)$ are asymmetric.

Based on the experimental result of the single π rotation, we perform multiple π rotations in the spin-wave basis. Figure 4(a) is the time sequences of the multiple π pulses. Figure 4(b) is the measured normalized retrieval efficiencies N_R and N_L versus the π-pulse number n. The results show that multiple rotations of the spin-wave vector occur under the actions of the multiple π pulses. At $n = 2$ (with two π pulses applied), the normalized retrieval efficiency N_R reaches ~0.6, whereas, N_L is 0.01, which means that almost all the coherence population is transferred back to spin wave $\vec{S}_{1,1}(z,t)$. As the π-pulse number n increases, the

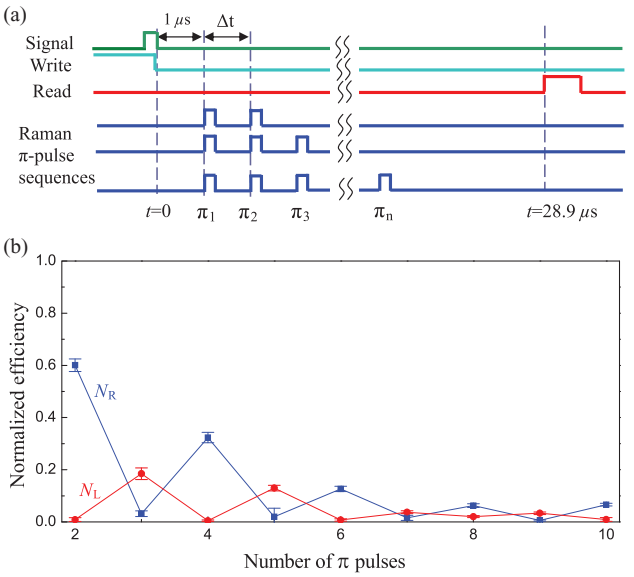

FIG. 4. (Color online) Multiple π rotations of the spin-wave vector under the actions of the multiple π pulses. (a) Time sequences of the multiple π pulses, π_i denotes the ith π pulse. $\Delta t = 1$ μs is the time delay between two successive pulses. (b) Blue square (red circular) points: the measured normalized retrieval efficiency $N_R(N_L)$.

normalized retrieval efficiency becomes smaller, which results from the coherence loss during the n π-pulse operations of the spin waves. After six π rotations, the normalized retrieval efficiency reduces to 0.15. At $n = 4$, the retrieval efficiency N_R is clearly larger than N_L at $n = 3$, that is because the retrieval efficiency from $\vec{S}_{-1,1}(z,t)$ is less than that from $\vec{S}_{1,1}(z,t)$.

Successively, a Ramsey interference experiment is performed in which two Raman laser pulses with a variable separate time τ_R are applied. For achieving a $\pi/2$ Raman pulse, the temporal length of the Raman laser pulses is set at $\sim$50 ns, and the peak power of the Raman pulse is still kept at $P = 80$ mW. The first $\pi/2$ pulse is applied at $t = 1$ μs, which rotates the initial spin wave $\vec{S}_{\Phi,1}(z,t_0) = \langle|\tilde{\rho}_{1,1}(z,t_0)|\rangle\binom{1}{0}$ into the superposition $\vec{S}_{\Phi,1}(z,t) = \frac{1}{\sqrt{2}}\langle|\tilde{\rho}_{1,1}(z,t_0)|\rangle\binom{1}{1}$. After a variable time interval τ_R the spin wave evolves into $\vec{S}_{\Phi,1}(z,t) = \frac{1}{\sqrt{2}}\langle|\tilde{\rho}_{1,1}(z,t_0)|\rangle\binom{e^{-i\Omega_L\tau_R}}{1}$ due to the Larmor precession with a precession frequency Ω_L, and then the second $\pi/2$ pulse is applied. We use scheme I to read spin waves $\vec{S}_{-1,1}(z,t)$ and $\vec{S}_{1,1}(z,t)$ at time $T = 28.9$ μs. Figure 5 plots the measured relative retrieval signal $N_{R(L)}$ as the function of interval τ_R. The solid lines are the fits to the data $N_{R(L)}$ using the sinusoidal functions $a(1 + b\ \cos\ 2\pi\tau_R/T_L)/2$ and $\zeta a(1 - b\ \cos\ 2\pi\tau_R/T_L)/2$ from which we obtain the Larmor period $T_L = 2.6 \times 10^{-6}$s and the Ramsey fringe contrast $b = 0.9$ for $N_{R(L)}$.

We have also investigated the transverse decay of the two spin waves by performing a Ramsey spectroscopy. The first and second $\pi/2$ pulses are applied at times t_1 and t_2, respectively [see the time sequence in Fig. 6(a)].

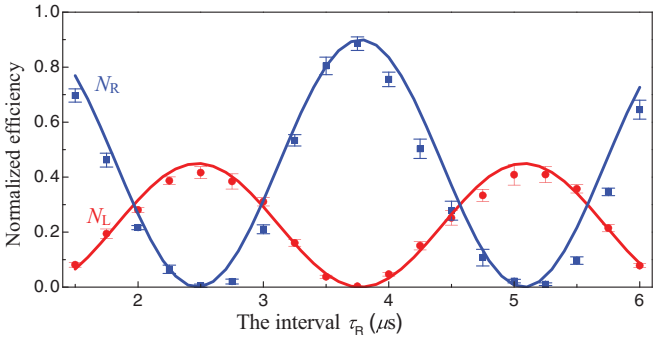

FIG. 5. (Color online) Ramsey fringes for a pair of $\pi/2$ pulses with a variable separate time τ_R (μs). Blue square (red circular) points: the normalized retrieval efficiency $N_{R(L)}$. The solid lines are sinusoidal fits to the data.

Subsequently, we switch on the σ^--polarized reading beam to retrieve the manipulated spin waves [see reading scheme I in Fig. 1(c)]. The retrieval signals $n_R = \int\langle|\hat{\varepsilon}_R^{\rm out}(z,t)|\rangle^2 dt$ and $n_L = \int\langle|\hat{\varepsilon}_L^{\rm out}(z,t)|\rangle^2 dt$ as the function of the time delay of $\tau_R = t_2 - t_1$ are shown in Fig. 6(b), which present damped sinusoidal oscillation. We can see, as increasing time delay τ_R, the contrast of the Ramsey fringes reduces. Fitting the data n_R and n_L to functions $Ae^{-\tau_R/T_1}(1 + b\ \cos\ 2\pi\tau_R/T_L)/2$ and $Be^{-\tau_R/T_1}(1 - b\ \cos\ 2\pi\tau_R/T_L)/2$, respectively, we have the $1/e$ decoherent time of $T_1 = 90$ μs and the contrast of the Ramsey fringes $b = e^{-\tau_R/T_2}$ with the $1/e$ decay time of $T_2 = 180$ μs. The decoherence of the spin waves on the time scale of T_1 (longitudinal) is induced by the atomic random motions [35]. The decay of the Ramsey contrast on the time

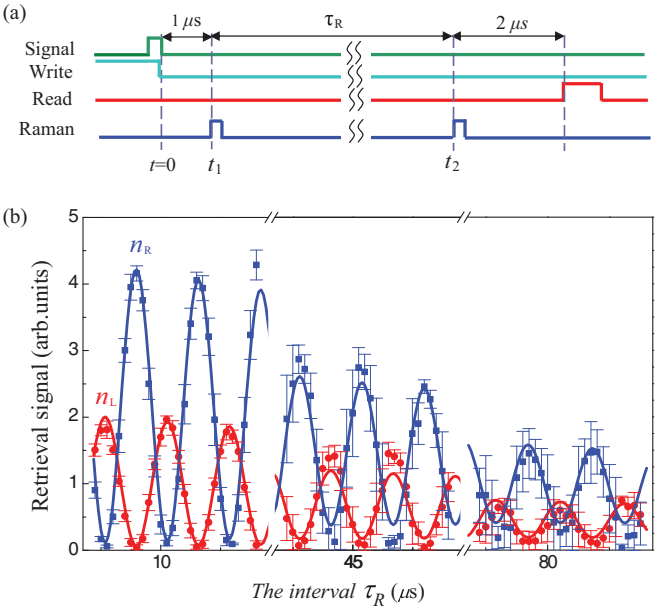

FIG. 6. (Color online) (a) Time sequence of two Raman $\pi/2$ pulses. (b) Ramsey fringes for a pair of $\pi/2$ pulses with a longer variable separate time τ_R (μs). Blue square (red circular) points are the retrieval signal $n_{R(L)}$, and the solid lines are exponential fits to the data. Note the breaks on the horizontal axis.

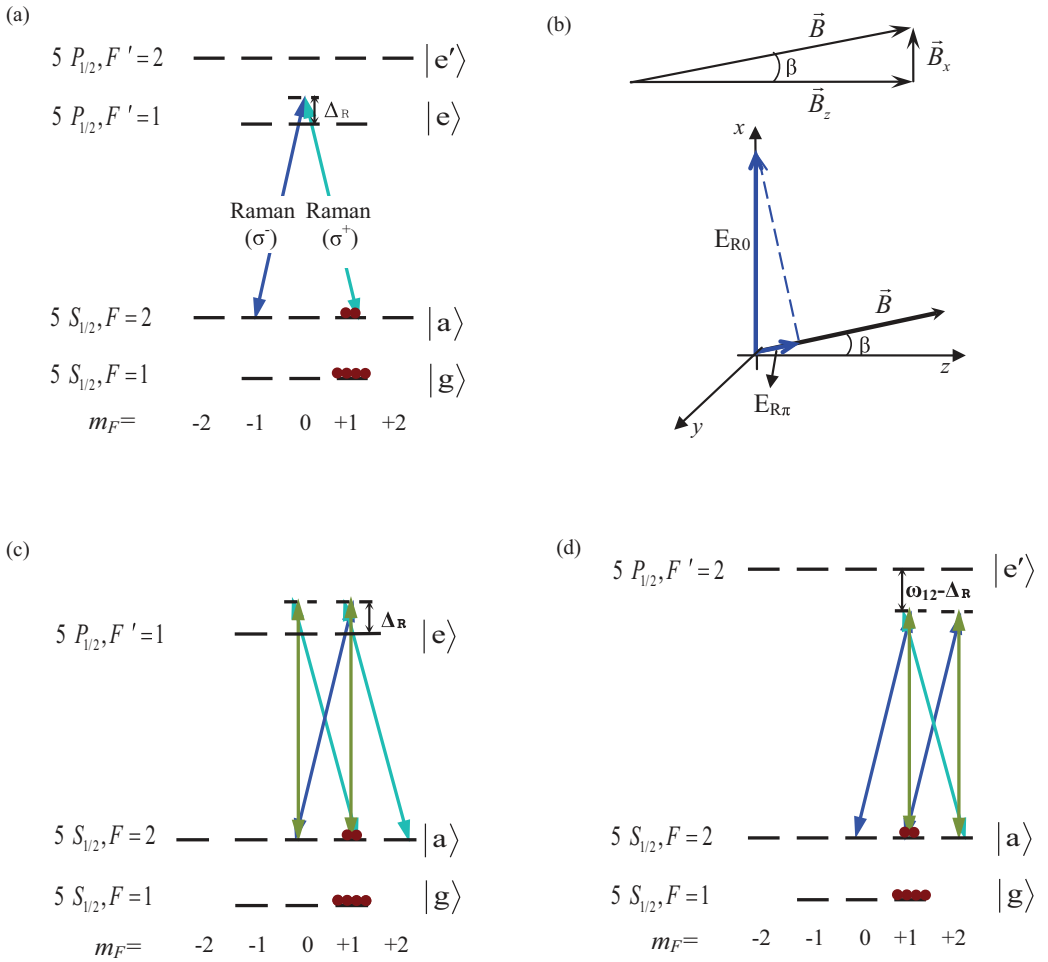

FIG. 7. (Color online) (a) Schematic of the relevant levels for stimulated Raman transitions. (b) Diagrams of the vectors of the magnetic fields (B, B_z, and B_x) and optical fields (E_R and $E_{R\pi}$). (c) Schematic of the three unwanted Raman transitions $|a_{m_F=1}\rangle \leftrightarrow |a_{m_F=0}\rangle$ through $|e_{m_F=0}\rangle$ and $|e_{m_F=1}\rangle$, respectively, as well as $|a_{m_F=1}\rangle \leftrightarrow |a_{m_F=2}\rangle$ through $|e_{m_F=1}\rangle$. (d) Schematic of the three unwanted Raman transitions $|a_{m_F=1}\rangle \leftrightarrow |a_{m_F=0}\rangle$ through $|e'_{m_F=1}\rangle$ as well as $|a_{m_F=1}\rangle \leftrightarrow |a_{m_F=2}\rangle$ though $|e'_{m_F=1}\rangle$ and $|e'_{m_F=2}\rangle$, respectively.

scale T_2 (transverse) arises from the random phase between the two spin waves, which is induced by the fluctuation of the magnetic field along $\hat{z}$.

V. DISCUSSION ON THE PHYSICAL REASONS FOR THE DECOHERENCE OF THE SPIN WAVE DURING RAMAN TRANSFERS

For a Raman π rotation, we obtain a transfer efficiency of ~78.4% in Fig. 3(a), which corresponds to a loss of spin wave of ~21.6%. In the following, the dominant physical reasons resulting in the decoherence of spin waves are discussed, and the possible methods to suppress the decoherence are analyzed briefly.

(1) The spontaneous photon scattering during a Raman π rotation. When the $\sigma^{\pm}$ components of the Raman laser drive transitions $|a_{m_F=\pm1}\rangle \leftrightarrow |e_{m_F=0}\rangle$ (with a detuning $\Delta_1 = \Delta_R$) and $|a_{m_F=\pm1}\rangle \leftrightarrow |e'_{m_F=0}\rangle$ (with a detuning $\Delta_2 = \omega_{12} - \Delta_R$) of the atoms, respectively, they will have small probabilities to be excited into states $|e_{m_F=0}\rangle$ and $|e'_{m_F=0}\rangle$ [36], which are given by

$$P_{e_0} = \frac{P_1\Omega_+^2}{\Delta_R^2} + \frac{P_{-1}\Omega_-^2}{\Delta_R^2} = \frac{\Omega_{R0}^2}{\Delta_R^2}(P_1 + P_{-1}), \quad (13a)$$

$$P_{e'_0} = \frac{P_1\Omega'^{\,2}_+}{(\omega_{12}-\Delta_R)^2} + \frac{P_{-1}\Omega'^{\,2}_-}{(\omega_{12}-\Delta_R)^2} = \frac{\Omega_{R0}^2}{(\omega_{12}-\Delta_R)^2}(P_1 + P_{-1}), \quad (13b)$$

respectively, where $P_1 = \langle\tilde{\rho}_{a_{m_F=1},a_{m_F=1}}\rangle$ and $P_{-1} = \langle\tilde{\rho}_{a_{m_F=-1},a_{m_F=-1}}\rangle$ are the atomic populations in states $|a_{m_F=1}\rangle$ and $|a_{m_F=-1}\rangle$, corresponding to the populations of spin waves $\vec{S}_{1,1}$ and $\vec{S}_{-1,1}$, respectively. As shown in Fig. 7(a), the σ^+ (σ^-) component of the Raman laser also drives transition $|a_{m_F=-1}\rangle \leftrightarrow |e'_{m_F=-2}\rangle(|a_{m_F=1}\rangle \leftrightarrow |e'_{m_F=2}\rangle)$ with a detuning $\Delta_2 = \omega_{12} - \Delta_R$ and a resonant Rabi frequency $\Omega_{-1,-2}(\Omega_{1,2})$, thus, a probability $P_{e'_{-2}} = \frac{P_{-1}\Omega^2_{-1,-2}}{(\omega_{12}-\Delta_R)^2}(P_{e'_2} = \frac{P_1\Omega^2_{+1,+2}}{(\omega_{12}-\Delta_R)^2})$ in states $|e'_{m_F=-2}\rangle(|e'_{m_F=2}\rangle)$ will be excited. According to the data for the Rb atom given in Ref. [29], we have $\Omega^2_{-1,-2} = \Omega^2_{1,2} = \frac{2}{3}\Omega^2_{R,0}$.

The atoms in excited states $|e_{m_F=0}\rangle, |e'_{m_F=0}\rangle, |e'_{m_F=-2}\rangle$, and $|e'_{m_F=2}\rangle$ will spontaneously scatter photons. The total scattering rate of the spontaneous photons from the Raman beam is [36]

$$R_{SE} = \gamma\left(P_{e_0} + P_{e'_0} + P_{e'_{-2}} + P_{e'_2}\right) = \gamma\Omega_{R,0}^2\left(\frac{1}{\Delta_R^2} + \frac{5/3}{(\omega_{12}-\Delta_R)^2}\right)(P_1 + P_{-1}), \quad (14)$$

where γ is the natural linewidth of the $5P_{1/2}$ levels. The time for a π rotation is $\tau_\pi = \frac{\pi}{2\Omega_R}$ [for the definition of Ω_R, see Eq. (5)]. The probability of spontaneous emissions from each atom in the interaction region for a π rotation equals [36]

$$P_{SE} = \frac{R_{SE}\tau_\pi}{(P_1 + P_{-1})} = \frac{\pi\gamma}{2\omega_{12}}\frac{5\Delta_R^2/3 + (\omega_{12}-\Delta_R)^2}{\Delta_R(\omega_{12}-\Delta_R)}. \quad (15)$$

For the presented experiment, $\Delta_R = 300$, $\omega_{12} = 816$, and $\gamma \approx 5.8$ MHz, we obtain $P_{SE} = 0.03$, which corresponds to a loss of the spin waves of 3% for a π rotation. To further reduce the loss of the spin waves, one may take very large detunings $\Delta_{1(}\Delta_2)$. For example, if $\Delta_1 \approx -3$ and $\Delta_2 \approx -3.8$GHz, the scattering probability P_{SE} will be less than 0.1%.

(2) The decoherence resulting from the unwanted Raman transfer. In the presented experimental setup, the input optical signal field propagates along $\hat{z}$, so we apply a magnetic field of $\vec{B} = B_z\hat{z}$ to make the quantization axis also along $\hat{z}$. However, due to imperfect compensation to the environmental magnetic fields, in a practical system there is a stray magnetic field $\vec{B}' = B_x\hat{x}$ around the atomic ensemble ($\hat{x}$ is the unit vector in the vertical direction [see Fig. 7(b)]). Thus, the quantization axis is actually along the effective magnetic field $\vec{B}_{\text{eff}} = B_z\hat{z} + B_x\hat{x}$, and there is an angle $\beta = \arctan(B_x/B_z)$ between the quantization axis ($\vec{B}_{\text{eff}}$) and $\hat{z}$. Since the $\hat{x}$-polarized Raman laser beam goes through the atoms in the $\hat{z}-\hat{y}$ plane ($\hat{y}$ is the unit vector in the horizontal direction), the projection of the $\hat{x}$-polarized Raman laser field $E_R(t)$ onto the direction of the magnetic field $\vec{B}_{\text{eff}}$ can be written as $\vec{E}_{R\pi}(t) = \vec{E}_R(t)\sin\beta$ [see Fig. 7(b)], which couples the π transitions $|5S_{1/2}, F = 2, m_F\rangle \leftrightarrow |5P_{1/2}, F' = 1, m'_F = m_F\rangle (m_F = 0, \pm 1)$ with a detuning Δ_R [Fig. 7(c)] as well as the π transitions $|5S_{1/2}, F = 2, m_F\rangle \leftrightarrow |5P_{1/2}, F' = 2, m'_F = m_F\rangle (m_F = \pm 1, \pm 2)$ with a detuning $\omega_{12} - \Delta_R$ [Fig. 7(d)]. The above-mentioned couplings and the couplings between the Raman fields $E_{R\pm}(t)$ and the $\sigma^\pm$ transitions [see Figs. 7(c) and 7(d)] induce Raman transfers between states $|a_{m_F=1}\rangle$ and $|a_{m_F=0}\rangle (|a_{m_F=2}\rangle)$, which will cause the spin-wave loss. For simplicity and without losing generality, we assume that the spin-wave excitations are in collective state $|a_{m_F=1}\rangle$ before the Raman transfer in the following calculations. In this case, there are six unwanted Raman two-photon transitions, which are $|a_{m_F=1}\rangle \leftrightarrow |a_{m_F=0}\rangle$ through $|e_{m_F=0}\rangle$ and $|e_{m_F=1}\rangle$, respectively, $|a_{m_F=1}\rangle \leftrightarrow |a_{m_F=2}\rangle$ through $|e_{m_F=1}\rangle$[see Fig. 7(c)], $|a_{m_F=1}\rangle \leftrightarrow |a_{m_F=0}\rangle$ through $|e'_{m_F=1}\rangle$, and $|a_{m_F=1}\rangle \leftrightarrow |a_{m_F=2}\rangle$ through $|e'_{m_F=1}\rangle$ and $|e'_{m_F=2}\rangle$ [see Fig. 7(d)], respectively. The total Raman-Rabi frequency for the two-photon transitions $|a_{m_F=1}\rangle \leftrightarrow |a_{m_F=0}\rangle$ and $|a_{m_F=1}\rangle \leftrightarrow |a_{m_F=2}\rangle$ is

$$\Omega_{1\to0} = 2\Omega_{R,0}^2 \sin\beta\left[\frac{1}{\Delta_R}\left(\sqrt{\frac{4}{3}} + \sqrt{\frac{1}{3}}\right) + \frac{1/\sqrt{3}}{\omega_{12}-\Delta_R}\right], \quad (16a)$$

and

$$\Omega_{1\to2} = 2\Omega_{R,0}^2 \sin\beta\left[\frac{\sqrt{2}}{\Delta_R} + \frac{1}{\omega_{12}-\Delta_R}\left(\sqrt{\frac{2}{9}} + \sqrt{\frac{8}{9}}\right)\right], \quad (16b)$$

respectively. The Raman transfer efficiencies for these two two-photon transitions are $T_{1\to0} = \sin^2\Omega_{1\to0}\tau_\pi$ and $T_{1\to2} = \sin^2\Omega_{1\to2}\tau_\pi$, respectively. Taking $\beta = \arctan(17/300) \approx 3.2^\circ$ and $\Delta_R = 300$ and $\omega_{12} = 816$ MHz, we obtain $T_{1\to0} = 5.3\%$ and $T_{1\to2} = 6.1\%$, respectively, which produce a total loss of spin waves of ~11.4%. If angle β can be reduced by precisely compensating the environmental magnetic field, the loss of spin waves will also decrease. Such as, when the residual magnetic field $\vec{B}'$ is reduced to ~2 mG, the estimated loss of the spin waves for a Raman π rotation will be less than ~0.16%.

Based on the above-discussed decoherence mechanisms, the estimated total loss of spin waves is ~14.4% for a Raman π rotation, which is lower than the experimentally measured value (~21.6%). Certainly, there are some complex and unclear loss mechanisms in the experimental system, which need to be explored further.

VI. CONCLUSION

In conclusion, using Raman laser pulses we experimentally demonstrated fast and multiple manipulations of two spin-wave excitations. The time scale of the π rotation in the spin-wave basis is ~100 ns, which is much less than the storage lifetime of the spin waves (90 μs). The measured Raman transfer efficiency for a Raman π rotation is ~78.4%, corresponding to a loss of spin waves of ~21.6%. The loss results from the decoherence of spin waves induced by Raman manipulations. The dominant decoherence mechanisms and the possible ways for reducing the decoherence are briefly discussed. By observing Ramsey fringes, we measure the dephasing time of the two spin waves, which is about ~180 μs. The dephasing is induced by the fluctuation in the environmental magnetic field and may be reduced by means of the dynamical decoupling scheme [22]. The presented manipulation method can be used for implementing single-qubit gate operations and the dynamical decoupling of qubit memory in atomic ensembles, which would be important in QIP based on an atomic ensemble.

ACKNOWLEDGMENTS

We acknowledge funding support from the 973 Program (Grant No. 2010CB923103) and the National Natural Science Foundation of China (Grants No. 10874106, No. 11274211, and No. 61121064).

[1] N. Sangouard, C. Simon, H. de Riedmatten, and N. Gisin, Rev. Mod. Phys. **83**, 33 (2011).

[2] L. M. Duan *et al*., Nature (London) **414**, 413 (2001).

[3] A. I. Lvovsky, B. C. Sanders, and W. Tittel, Nat. Photonics **3**, 706 (2009).

[4] L.-M. Duan, J. I. Cirac, and P. Zoller, Phys. Rev. A **66**, 023818 (2002).

[5] T. Chanelière, D. N. Matsukevich, S. D. Jenkins, S.-Y. Lan, T. A. B. Kennedy, and A. Kuzmich, Nature (London) **438**, 833 (2005).

[6] U. Schnorrberger, J. D. Thompson, S. Trotzky, R. Pugatch, N. Davidson, S. Kuhr, and I. Bloch, Phys. Rev. Lett. **103**, 033003 (2009).

[7] R. Zhang, S. R. Garner, and L. V. Hau, Phys. Rev. Lett. **103**, 233602 (2009).

[8] L. Karpa, F. Vewinger, and M. Weitz, Phys. Rev. Lett. **101**, 170406 (2008).

[9] D. N. Matsukevich, T. Chanelière, M. Bhattacharya, S.-Y. Lan, S. D. Jenkins, T. A. B. Kennedy, and A. Kuzmich, Phys. Rev. Lett. **95**, 040405 (2005).

[10] S. Chen, Y.-A. Chen, B. Zhao, Z.-S. Yuan, J. Schmiedmayer, and J.-W. Pan, Phys. Rev. Lett. **99**, 180505 (2007).

[11] Y. O. Dudin, S. D. Jenkins, R. Zhao, D. N. Matsukevich, A. Kuzmich, and T. A. B. Kennedy, Phys. Rev. Lett. **103**, 020505 (2009).

[12] H. Tanji, S. Ghosh, J. Simon, B. Bloom, and V. Vuletić, Phys. Rev. Lett. **103**, 043601 (2009).

[13] K. S. Choi *et al*., Nature (London) **452**, 67 (2008).

[14] Y.-W. Cho and Y.-H. Kim, Opt. Express **18**, 25786 (2010).

[15] D. G. England, P. S. Michelberger, T. F. M. Champion, K. F. Reim, K. C. Lee, M. R. Sprague, X.-M. Jin, N. K. Langford, W. S. Kolthammer, J. Nunn, and I. A. Walmsley, J. Phys. B **45**, 124008 (2012).

[16] L.-M. Duan, Phys. Rev. Lett. **88**, 170402 (2002).

[17] P. Dong, Z.-Y. Xue, M. Yang, and Z.-L. Cao, Phys. Rev. A **73**, 033818 (2006).

[18] D. J. Wineland, C. Monroe, W. M. Itano, D. Leibfried, B. E. King, and D. M. Meekhof, J. Res. Natl. Inst. Stand. Technol. **103**, 259 (1998).

[19] D. Schrader, I. Dotsenko, M. Khudaverdyan, Y. Miroshnychenko, A. Rauschenbeutel, and D. Meschede, Phys. Rev. Lett. **93**, 150501 (2004).

[20] L. Wang, X.-L. Song, A.-J. Li, H.-H. Wang, X.-G. Wei, Z.-H. Kang, Y. Jiang, and J.-Y. Gao, Opt. Lett. **33**, 2380 (2008).

[21] S. Li, Z. Xu, H. Zheng, X. Zhao, Y. Wu, H. Wang, C. Xie, and K. Peng, Phys. Rev. A **84**, 043430 (2011).

[22] G. S. Uhrig, Phys. Rev. Lett. **98**, 100504 (2007).

[23] M. Lettner, M. Mücke, S. Riedl, C. Vo, C. Hahn, S. Baur, J. Bochmann, S. Ritter, S. Dürr, and G. Rempe, Phys. Rev. Lett. **106**, 210503 (2011).

[24] M. Fleischhauer and M. D. Lukin, Phys. Rev. Lett. **84**, 5094 (2000).

[25] M. Fleischhauer and M. D. Lukin, Phys. Rev. A **65**, 022314 (2002).

[26] M. D. Lukin, Rev. Mod. Phys. **75**, 457 (2003).

[27] For choosing an optimal detuning Δ_R to implement effective Raman transfers, we have observed the transfer efficiency as the function of the detuning Δ_R for a fixed Raman power of ∼80 mW. We find that the transfer efficiency will reach a maximum value of ∼78.4% when the detuning Δ_R is taken around: 300 MHz. So, we choose $\Delta_R = 300$ MHz to perform the Raman transfers.

[28] W. C. Campbell, J. Mizrahi, Q. Quraishi, C. Senko, D. Hayes, D. Hucul, D. N. Matsukevich, P. Maunz, and C. Monroe, Phys. Rev. Lett. **105**, 090502 (2010).

[29] http://steck.us/alkalidata/.

[30] K. Surmacz, J. Nunn, K. Reim, K. C. Lee, V. O. Lorenz, B. Sussman, I. A. Walmsley, and D. Jaksch, Phys. Rev. A **78**, 033806 (2008).

[31] A. V. Gorshkov, A. André, M. D. Lukin, and A. S. Sørensen, Phys. Rev. A **76**, 033805 (2007).

[32] A. Joshi and M. Xiao, Phys. Rev. A **71**, 041801(R) (2005).

[33] H. Wang, S. Li, Z. Xu, X. Zhao, L. Zhang, J. Li, Y. Wu, C. Xie, K. Peng, and M. Xiao, Phys. Rev. A **83**, 043815 (2011).

[34] M. P. A. Jones, J. Beugnon, A. Gaëtan, J. Zhang, G. Messin, A. Browaeys, and P. Grangier, Phys. Rev. A **75**, 040301(R) (2007).

[35] B. Zhao, Y.-A. Chen, X.-H. Bao, T. Strassel, C.-S. Chuu, X.-M. Jin, J. Schmiedmayer, Z.-S. Yuan, S. Chen, and J.-W. Pan, Nat. Phys. **5**, 95 (2009).

[36] R. Ozeri, W. M. Itano, R. B. Blakestad, J. Britton, J. Chiaverini, J. D. Jost, C. Langer, D. Leibfried, R. Reichle, S. Seidelin, J. H. Wesenberg, and D. J. Wineland, Phys. Rev. A **75**, 042329 (2007).